crystals

MDPI

Communication

Synthesis and Characterization of Mechanically Alloyed Nanostructured (Ti,Cr)C Carbide for Cutting Tools Application

Mohsen Mhadhbi [1] and Wojciech Polkowski [2,*]

[1] Laboratory of Useful Materials, National Institute of Research and Physicochemical Analysis, Technopole Sidi Thabet, Ariana 2020, Tunisia
[2] Łukasiewicz Research Network—Krakow Institute of Technology, 30-418 Kraków, Poland
* Correspondence: wojciech.polkowski@kit.lukasiewicz.gov.pl; Tel.: +48-12-2618-324

Abstract: (Ti,Cr)C is a novel additive for high-performance cermets. In this work, a $(Ti_{0.8}Cr_{0.2})C$ nanostructured solid solution was synthesized via Mechanical Alloying (MA) from the mixture of of Ti, Cr, and C powders. The MA process was carried out at room temperature under argon atmosphere with a duration limited to 20 h. Phase changes and microstructure evolution of the powders during the MA process were characterized by X-ray diffraction (XRD), scanning electron microscopy (SEM), and transmission electron microscopy (TEM) techniques. The results of XRD analysis demonstrated the synthesis of (Ti,Cr)C solid solution with a crystallite size of about 10 nm that were micro-strained to about 1.34%. The crystallite size displays a decreasing trend with increasing milling time. The results of direct observations of structural features by TEM method in 20 h MAed samples shows a good agreement with the results from the XRD analyses.

Keywords: Nano (Ti,Cr)C powder; mechanical alloying (MA); nanostructure; X-ray diffraction

Citation: Mhadhbi, M.; Polkowski, W. Synthesis and Characterization of Mechanically Alloyed Nanostructured (Ti,Cr)C Carbide for Cutting Tools Application. *Crystals* **2022**, *12*, 1280. https://doi.org/10.3390/cryst12091280

Academic Editor: Umberto Prisco

Received: 16 August 2022
Accepted: 7 September 2022
Published: 9 September 2022

1. Introduction

Titanium carbide (TiC) is widely used in industrial applications as a hard coating to protect the surface of cutting tools from wear and erosion, resulting in an extended tool life [1]. It exhibits high strength, high hardness, good wear resistance, high melting point, high chemical stability, and low friction coefficient [2–5]. In particular, nanosized TiC particles are considered as promising microstructural modifiers and mechanical strengtheners for particle dispersed composite alloys, since fine TiC dispersoids in the metallic matrix improve the overall properties of the materials without an adverse effect on their ductility or toughness [6,7].

So far, several methods have been used to prepare nanostructured carbides including a carbothermal reduction [8], mechanical alloying (MA) [9], spark plasma sintering (SPS) [10], chemical vapor deposition (CVD) [11], etc. Among the aforementioned techniques, the MA is an easy and cost-efficient route usually used to prepare nanostructured materials, and especially for manufacturing composite powders [12].

As described in literature reports, the main idea behind using a (Ti,*M*)C (*M* = transition refractory metal) solid solution instead of TiC is to improve the toughness of cermets. Park and Kang [13] have synthesized nanocrystalline $(Ti_{1-x}W_x)C$ solid solutions, with a homogenous microstructure and improved properties by the SPS process. Kim et al. [14] fabricated homogeneous (Ti,W)C nanocomposite powders by a high-energy ball milling of a mixture of Ti, W, and C powders. The obtained nanopowders were then SPSed to receive fully densified sinters having a uniform microstructure with a mean grain size of 500 nm. Kwon et al. [15] prepared (Ti,V)C solid solution powders by the MA of Ti-V alloy and graphite powder mixture. The MA process was carried out in a high-energy planetary ball mill for up to 20 h under an argon atmosphere. Additionally, Bandyopadhyay et al. [16] investigated the effect of Ti substitution by W on the microstructure of the $Ti_{0.9}W_{0.1}C$ carbide. They reported that TiWC alloy was formed after 50 min of milling and a fully

nanocrystalline single phase cubic $Ti_{0.9}W_{0.1}C$ compound with a particle size of 11 nm was formed after 8 h of milling. Hence, the effect of ball milling on microstructural change of (Ti,W)C solid solution was experimentally studied by Yang et al. [17]. They found that with increasing milling time up to 108 h, the initial crystallite size decreased from 38.6 to 19.2 nm. Analogously, Dutta et al. [18] reported the formation of $Ti_{0.9}Al_{0.1}C$ nano-carbide after 3 h of milling. They found that that the results of crystal structure examinations obtained by TEM technique are in a good agreement with those derived from the XRD measurements. Wang et al. [19] also produced a (Ti, Mo)C carbide reinforced Fe-based surface composite coating by the laser cladding technique. It has been concluded that (Ti, Mo)C particles with the FCC structure and various shapes are obtained after the solidification. Recently, Yildiz et al. [20] prepared via the SPS a novel multi-component (Ti,Zr,Hf,W)C ceramic with a nano-hardness of 32.7 GPa and a fracture toughness of 5 MPa $m^{1/2}$. Recently, Vorotilo et al. [21] proposed that a solid solution (Ti,Cr)C, while retaining the main advantages of TiC, possesses higher oxidation resistance owing to the formation of Cr_2O_3. The (Ti,Cr)C cermets have been produced by a combustion synthesis driven by the Self-propagated High Temperature Synthesis (SHS) [21] or by High-Velocity Air Plasma Spraying [22]. However, to our best knowledge, there are no available reports on the MA synthesis of this type of solid solution-based cermet. Therefore, by taking into account a documented feasibility of the SPS process in a fabrication of high performance cermets, as well as a high impact of the batch powders on the resulted properties of final sinters; the main goal of our this work is to obtain a $(Ti_{0.8}C_{0.2})C$ composite powder with a suitable particle size that can be employed in the SPS process. Specifically, we are showing for the first time the results of systematic studies on the effect of milling time on the structural evolution of a novel mechanically alloyed $(Ti_{0.8}Cr_{0.2})C$ powders.

2. Materials and Methods

A mixture of elemental Ti (<40 μm, 99.9%, Prolabo, Bankgkok, Thailand), carbon (5 μm, 99.9%, Fischer Scientific, Waltham, MA, USA) and chromium (100–300 μm, 99.9%, ACROS, Boston, MA, USA) powders was sealed into a stainless-steel vial (having a volume of 45 mL) with 5 stainless steel balls (15 mm in diameter and 14 g in mass each) in a glove box filled with purified argon to prevent oxidation. The ball to powder weight ratio was 70:1. The mechanical alloying (MA) procedure of up to 20 h was performed at room temperature using a high-energy ball mill (Fritsch Pulverisette 7 planetary mill, Weimar, Germany), as shown in Figure 1.

Figure 1. P7 planetary ball mill and milling media used in the experiments.

The crystalline properties of the powders were characterized by the XRD method, by using a Panalytical XPERT PRO MPD (Cambridge, UK) diffractometer with CuK_{α} radiation. The existing phases were determined by the High Score Plus program based on the ICDD PDF2 data base, while a crystallite size was determined from acquired diffraction data by the FullProf program (Saclay, France) [23] employing the Rietveld method [24]. The morphology of powders was investigated by scanning electron microscopy (SEM, JEOL JSM-5400 model, Tokyo, Japan) coupled with energy dispersive X-ray analysis (EDX). The transmission electron microscopy (TEM) was used for the investigation of internal nanostructure of powders. The structural analysis was complemented by using FEI Tecnai G2 high-resolution TEM (Massachusetts, USA) operated at 200 kV with a spatial resolution of 1.9 Angstrom.

3. Results and Discussion

3.1. XRD Characterization

Figure 2a shows the XRD patterns of samples prepared by the MA after various milling times. The acquired XRD pattern of the un-milled powder mixture consists of Bragg diffraction peaks of Ti, Cr, and C. After 1 h 30 min of MA, all the carbon peaks disappeared totally, while the appearance of $TiCr_2$ peak and the reflections of Ti and Cr became broad without any shift in peak positions. Consequently, it is considered that the high-energy impact leads to the transformation of crystalline graphite into amorphous carbon (which is also supported by the literature reports [25,26]). After 3 h of MA, a disappearance of Cr peaks and appearance of (110) peak related to austenite iron (α-Fe) contamination resulted from the abrasive wear between vial and balls, was observed. When the MA time was extended to 5 h, the Ti peaks disappeared completely and the diffraction peaks were broadened and shifted into lower angles as a result of the formation of (Ti,Cr)C solid solution due to refinement of the grain size and the introduction of internal stresses. An analogous behavior was also reported in [27–29]. After continuing the MA for 10 h, the (Ti,Cr)C peaks broadened further due to the decrease in the crystallite sizes and an accumulation of lattice strains caused by fracturing and cold welding of the powder particles during the milling process. Between 10 and 20 h of MA, the structure remains almost unchanged: the (Ti,Cr)C solid solution maintains the NaCl type structure with a space group of Fm-3m. These results are similar to those reported by Shon et al. [30]. They have revealed that the average crystallite size of (Ti,Cr)C powders, obtained from the mixture of Ti-Cr alloy and graphite, MA for 20 h was about 34 nm. Figure 2b presents the Rietveld refinement plot of TiCrC powder after 20 h of the MA process. The calculated profile is represented by the black line, the observed profile by the red dots, and the difference pattern by the blue continuous line. The vertical lines (green) represent the positions of all possible Bragg reflections. The figure indicates that Cr substitutes Ti in the TiC matrix and consequently lead to a decrease in lattice parameter.

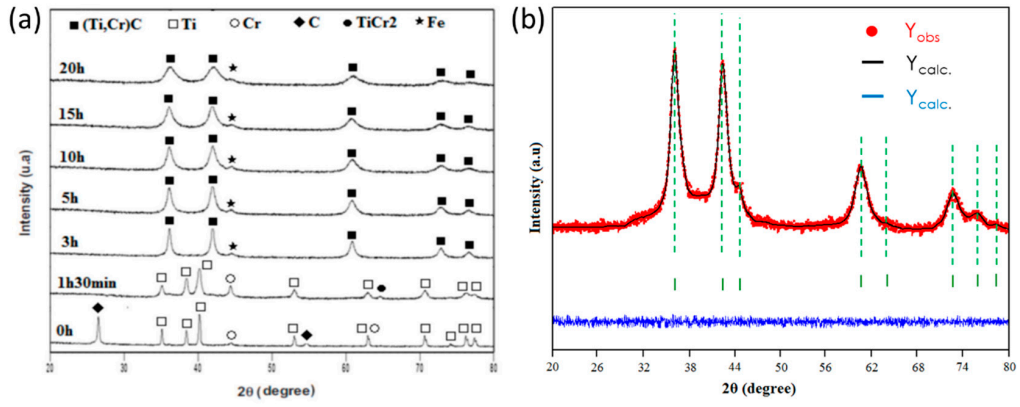

Figure 2. XRD patterns of samples prepared by MA for different milling times (**a**). Rietveld refinement plot of the sample milled for 20 h (**b**).

The quantitative analysis of microstructural parameters derived from Rietveld refinement of XRD patterns taken from samples MAed for different times, are illustrated in Table 1. It is found that the average crystallite size of (Ti, Cr)C decreases with increasing milling time, from 18 nm after 3 h of the MA and remain nearly constant (about 10 nm) for 15 and 20 h of MA. Thus, all identified phases, namely Ti, Cr, $TiCr_2$, (Ti,Cr)C and Fe, present the same behavior. This decrease can be explained by the refinement of structure and the creation of a large number of crystal defects, such as dislocations and stacking faults [31]. These findings are in line with reports by Zhu et al. [32] who have also connected a decrease in crystallite size with increased dislocation density; reflected as a broadening of XRD peaks. From these observations, it is evident that the reduced particle size plays significant role in inclusion of Cr atoms in TiC matrix. As it is listed in Table 1, the values of mean microstrains are higher for the (Ti, Cr)C phase as compared to other phases. Moreover, the average microstrain of (Ti, Cr)C increases with the MA time, from 0.25 ± 0.01% after 3 h of MA to reach 1.34 ± 0.04% after 20 h of MA. The increase of the microstrain with milling time is generated by the increase of dislocation density and grain boundary fraction, which due to severe plastic deformation generated from the high-energy induced during milling [33]. Furthermore, the calculated lattice parameter of (Ti, Cr)C, obtained from XRD data, decreased from 0.44169 to 0.43036 nm for the powder samples milled for 3 and 20 h, respectively. The value is consistent with that reported by Kwon et al. (a = 0.43075 nm) [34]. This suggest that the lattice parameter was decreased by the substitution of Cr because the atomic radius of Cr (166 pm) is smaller than that of Ti (176 pm) [35]. The decrease in lattice parameter can be explained by the substitution of Ti by Cr and, therefore, by the formation of the $Ti_{0.8}Cr_{0.2}C$ carbide. This finding is consistent with the reported literature for other similar compounds, like TiC_x, Cu-TiC_x, and $Cr_{2-x}M_xS_3$ (M = Ti, V, Sn) [36,37].

Table 1. The results of quantitative analysis of microstructural parameters derived from Rietveld refinement for XRD patterns of samples MA for different times.

MA Time (h)	Phase	Space Group	Lattice Parameter (nm)	Crystallite Size (nm)	Microstrain (%)
1.5	Ti	Fm-3m	a = 0.43281(4)	55	0.25 ± 0.01
	Cr	Im-3m	a = 0.29236(1)	40	0.94 ± 0.01
	$TiCr_2$	$P6_3/mmc$	a = 0.69011(3)	31	0.15 ± 0.01
3	(Ti,Cr)C	Fm-3m	a = 0.44169(5)	18	0.12 ± 0.02
	Fe	Im-3m	a = 0.2873(5)	17	0.21± 0.01
5	(Ti,Cr)C	Fm-3m	a = 0.44033(4)	15	0.25 ± 0.03
	Fe	Im-3m	a = 0.2874(3)	15	0.22 ± 0.01
10	(Ti,Cr)C	Fm-3m	a = 0.44949(4)	13	1.28 ± 0.04
	Fe	Im-3m	a = 0.2876(2)	13	0.23 ± 0.01
15	(Ti,Cr)C	Fm-3m	a = 0.43033(2)	11	1.33 ± 0.04
	Fe	Im-3m	a = 0.2877(5)	11	0.25 ± 0.01
20	(Ti,Cr)C	Fm-3m	a = 0.43036(3)	10	1.34 ± 0.04
	Fe	Im-3m	a = 0.2879(4)	11	0.26 ± 0.01

3.2. SEM Characterization

Figure 3 shows SEM micrographs of the $Ti_{0.8}Cr_{0.2}C$ powders after the MA for 5, 10, and 20 h. After 5 h of the MA, the grains are formed by an assembly of large particles exhibiting an irregular shape and having an average particle size of about 1–2 μm (Figure 3a). When the MA time was increased to 10 h, we observed significant particle refinement. The initial powders were transformed into fine particles with an average particle size of about 0.4 μm (Figure 3b). The MA up to 20 h results in a further particle size reduction and a formation of homogenous powders with fine and agglomerated particles having the average particle size less than 1 μm (Figure 3c). It is well accepted that the MA process leads to continuous cold welding, fracturing, and rewelding of powder particles [35]. Figure 3d shows an exemplary EDX spectrum acquired from the powder milled for 20 h. The results indicate

a presence of major elements (i.e., Ti, Cr, and C). In addition, the results of EDX analyzes revealed trace amounts of Fe, probably coming from the applied milling materials of balls and vial. Furthermore, the results of EDX analyses indicate that the carbide contains 47. 59 C, 40.49 Ti, 9.95 Cr, and 1.97 Fe (at.%). Thus, the alloying ratio is Ti:Cr:C = 0.82:0.201:1, which indicates that carbides may be $Ti_{0.8}Cr_{0.2}C$.

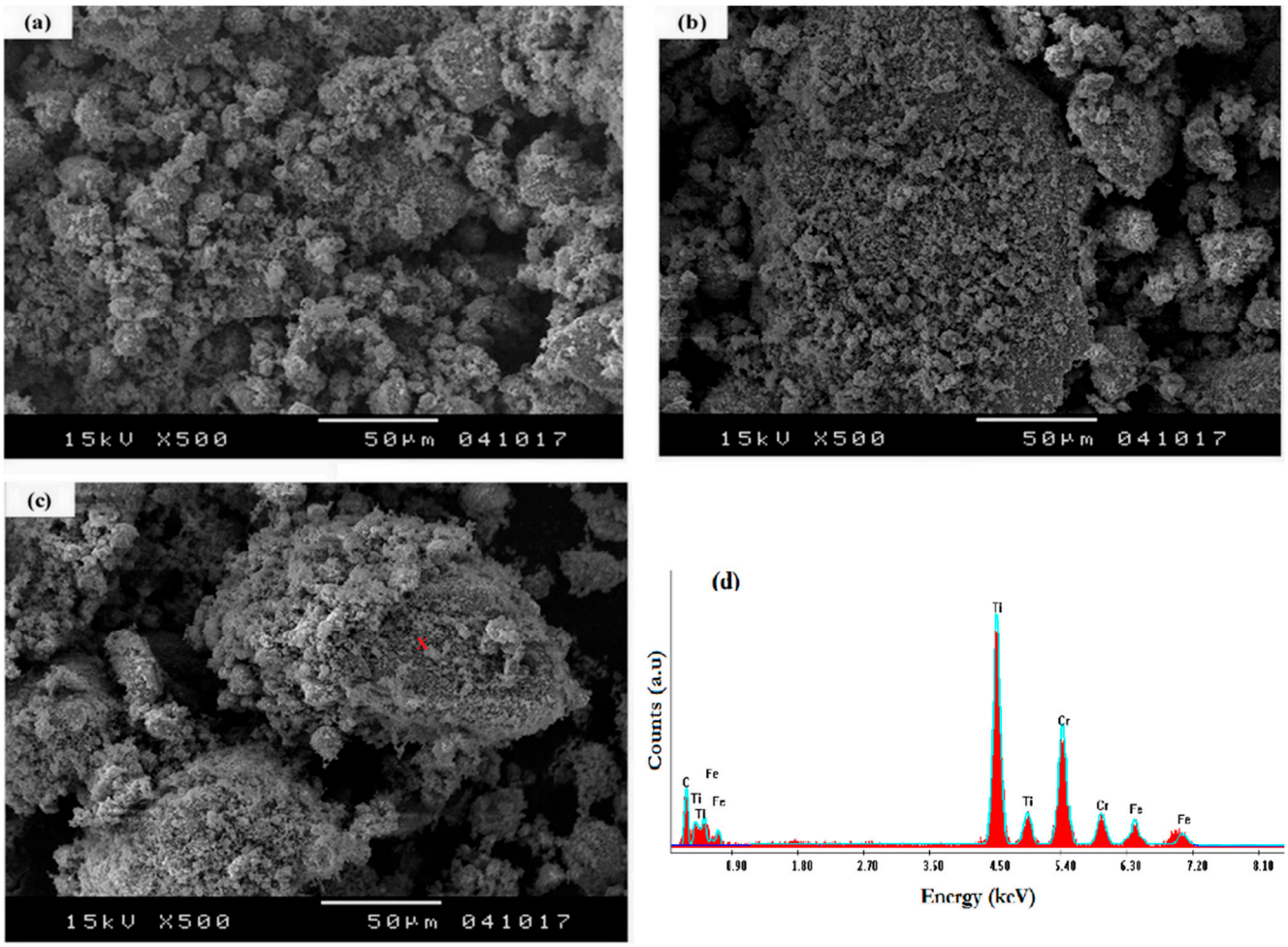

Figure 3. SEM micrographs of samples after MA for 5 h (**a**); 10 h (**b**); and 20 h (**c**). (**d**) An exemplary EDX spectrum taken form the sample milled for 20 h (zone marked with X).

3.3. TEM Characterization

Figure 4 shows a TEM micrograph and selected area electron diffraction (SAED) pattern of the sample after the MA for 20 h. Figure 4a reveals that the particle powders were irregular in shape, while the average size was refined to about 15 nm and the agglomeration was high. Therefore, the figure reveals the existence of many grains (i.e., the polycrystalline structure) in nanoscale powder particles. This result was in a good agreement with those obtained by the XRD method. Figure 4b shows the indexed SAED showing only the presence of cubic (Ti,Cr)C solid solution phase in the 20 h milled sample.

To summarize: based on our original experimental findings coming from the pioneering systematic studies, we confirm that a nanostructured (Ti,Cr)C solid solution having an adequate microstructural features and morphology to be applied in the SPS process, can be successfully obtained after 20 h of MA of Ti, Cr, and C elemental powders. The as-obtained nanopowders can be further consolidated through SPS in order to obtain a dense bulk (Ti,Cr)C nanocarbide with enhanced properties compared to TiC carbide. Thus, three parameters in terms of crystallite size, microstrain, and lattice parameter are obtained from XRD line profiles. The values are typical to these of batch powders for the SPS pro-

cess [36]. Thus, the milling time should be carefully selected taking to account the particle size and shape of the prepared powders. It can be observed that both crystallite size and lattice parameter decrease with increasing milling time, whereas the microstrain increases. These results are in a good agreement with the reference work [38]. As shown in the SEM images, the morphological evolution during the MA process includes three typical steps for a mechanical synthesis of multicomponent intermetallic/interstitial compounds, i.e., (i) a cold welding, (ii) a fracturing, and (iii) a rewelding between particles for longer milling times (between 15 and 20 h). Both applied diffraction-based techniques (TEM/SAED and XRD) confirmed the morphology and structure of MAed powders.

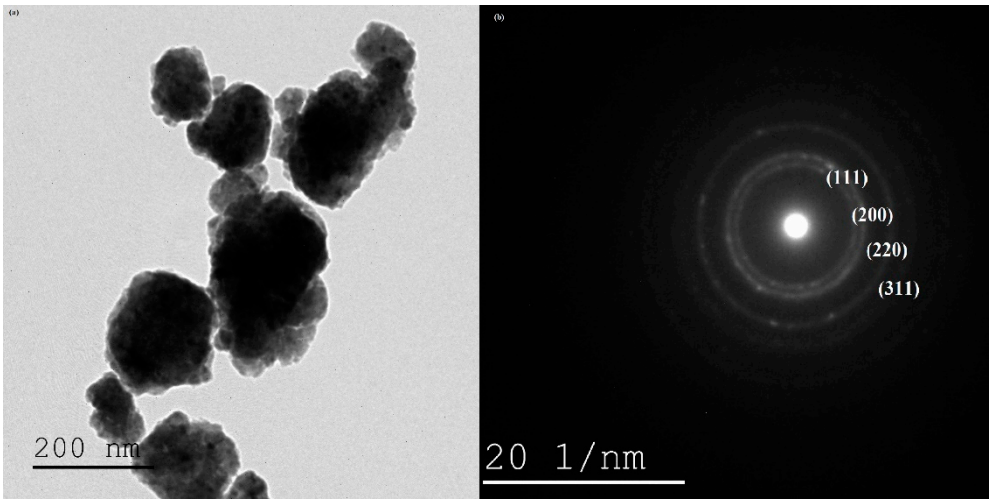

Figure 4. (**a**) HRTEM image and (**b**) SAED patterns of the powder after MA for 20 h.

4. Conclusions

Based on the results of the present study supported by a proper literature data, the following conclusions can be drawn:

1. Nanocrystalline solid solution (Ti,Cr)C with nano-sized crystallites was fabricated by mechanical alloying of Ti, Cr, and graphite elemental powders. The average grain size of the (Ti,Cr)C was 10 nm, and the average micro-strain was 1.34% for sample MA during 20 h.
2. The (Ti,Cr)C solid solution having a NaCl type structure and a space group of Fm-3m, was formed after 3 h of the MA process.
3. The crystallite size and the lattice parameter decrease by increasing milling time down to 10 nm and 0.43036 nm after 20 h of MA, respectively. This decrease can be attributed to the formation of crystal defects induced by high-energy ball milling. The microstrain increases with increasing milling time, which can be related to the strain-enhanced solubility of Cr in TiC matrix.
4. The crystallite size obtained from XRD is well correlated with the results of TEM analyses.

Author Contributions: M.M. have designed and performed the experiments. M.M. and W.P. have discussed and analyzed the data. M.M has written the draft version of manuscript. W.P. has edited the draft and prepared the final version of manuscript. All authors have read and agreed to the published version of the manuscript.

Funding: This research received no external funding.

Data Availability Statement: Raw experimental data are available on demand from M.M.

Acknowledgments: The authors would like to thank to all who have contributed to this work.

Conflicts of Interest: The authors declare no conflict of interest.

References

1. He, X.M.; Zhi, W.; Li, H.D. Investigation of TiC Films Synthesized by Low Energy Ion Bombardment. *J. Mater. Res.* **1994**, *9*, 2355–2361. [CrossRef]
2. Dong, Z.J.; Li, X.K.; Yuan, G.M.; Cui, Z.W.; Cong, Y.; Westwood, A. Tensile Strength, Oxidation Resistance and Wettability of Carbon Fibers Coated with a TiC Layer Using a Molten Salt Method. *Mater. Des.* **2013**, *50*, 156–164. [CrossRef]
3. Boonruang, C.; Thongtem, S. Fast Processing Technique for TiC Coatings on Titanium. *Chiang Mai J. Sci.* **2010**, *37*, 206–212.
4. Brama, M.; Rhodes, N.; Hunt, J.; Ricci, A.; Teghil, R.; Migliaccio, S.; Rocca, C.D.; Leccisotti, S.; Lioi, A.; Scandurra, M.; et al. Effect of Titanium Carbide Coating on the Osseointegration Response in Vitro and in Vivo. *Biomaterials* **2007**, *28*, 595–608. [CrossRef]
5. Saba, F.; Raygan, S.; Abdizadeh, H.; Dolatmoradi, A. Preparing TiC Coating on AISI D2 Steel Using Mechanical Milling Technique. *Powder Technol.* **2013**, *246*, 229–234. [CrossRef]
6. Lazarova, R.; Petrov, R.H.; Gaydarova, V.; Alexeev, A.; Manchev, M.; Manolov, V. Microstructure and Mechanical Properties of P265GH Cast Steel after Modification with TiCN Particles. *Mater. Des.* **2011**, *32*, 2734–2741. [CrossRef]
7. Han, Y.; Shi, J.; Xu, L.; Cao, W.Q.; Dong, H. TiC Precipitation Induced Effect on Microstructure and Mechanical Properties in Low Carbon Medium Manganese Steel. *Mater. Sci. Eng. A* **2011**, *530*, 643–651. [CrossRef]
8. Jung, J.; Kang, S. Sintered (Ti,W)C Carbides. *Scr. Mater.* **2007**, *56*, 561–564. [CrossRef]
9. Mhadhbi, M. Structural and Morphological Studies of Nanostructured TiC Powders Prepared by Mechanical Alloying. *Mod. App. Mater. Sci.* **2021**, *3*, 445–450. [CrossRef]
10. Liu, S.; Hu, W.; Xiang, J.; Wen, F.; Xu, B.; Yu, D.; He, J.; Tian, Y.; Liu, Z. Mechanical Properties of Nanocrystalline TiC-ZrC Solid Solutions Fabricated by Spark Plasma Sintering. *Ceram. Int.* **2014**, *40*, 10517–10522. [CrossRef]
11. Hayashi, M.; Mamyouda, T.; Habuka, H.; Ishiguro, A.; Ishii, S.; Daigo, Y.; Ito, H.; Mizushima, I.; Takahashi, Y. Design of a Silicon Carbide Chemical Vapor Deposition Reactor Cleaning Process Using Chlorine Trifluoride Gas Accounting for Exothermic Reaction Heat. *ECS J. Solid State Sci. Technol.* **2020**, *9*, 104008. [CrossRef]
12. Suryanarayana, C. Mechanical Alloying and Milling. *Prog. Mater. Sci.* **2001**, *46*, 1–184. [CrossRef]
13. Park, S.; Kang, S. Toughened Ultra-fine (Ti,W)(CN)-Ni Cermets. *Scr. Mater.* **2005**, *52*, 129–133. [CrossRef]
14. Kim, Y.K.; Shim, J.H.; Yang, H.S.; Park, J.K. Mechanochemical Synthesis of Nanocomposite Powder for Ultrafine (Ti, Mo)C-Ni Cermet Without Core-rim Structure. *Int. Ref. Met. Hard. Mater.* **2004**, *22*, 193–196. [CrossRef]
15. Kwon, H.; Jung, S.A.; Suh, C.Y.; Roh, K.M.; Kim, W. Mechanical Properties of (Ti,V)C-Ni Composite Prepared Using Ultrafine Solid-Solution (Ti,V)C Phase. *Ceram. Int.* **2014**, *40*, 12579–12583. [CrossRef]
16. Bandyopadhyay, S.; Dutta, H.; Pradhan, S.K. XRD and HRTEM Characterization of Mechanosynthesized $Ti_{0.9}W_{0.1}C$ Cermet. *J. Alloys Compd.* **2013**, *581*, 710–716. [CrossRef]
17. Yang, M.; Guo, Z.; Xiong, J.; Liu, F.; Qi, K. Microstructural Changes of (Ti,W)C Solid Solution Induced by Ball Milling. *Int. Refract. Met. Hard Mater.* **2017**, *66*, 83–87. [CrossRef]
18. Dutta, H.; Sen, A.; Pradhan, S.K. Microstructure Characterization of Ball-mill Prepared Ternary $Ti_{0.9}Al_{0.1}C$ by X-ray Diffraction and Electron Microscopy. *J. Alloys Compd.* **2010**, *501*, 198–203. [CrossRef]
19. Wang, X.; Zhang, M.; Qu, S. Development and Characterization of (Ti, Mo)C Carbides Reinforced Fe-based Surface Composite Coating Produced by Laser Cladding. *Opt. Lasers Eng.* **2010**, *48*, 893–898. [CrossRef]
20. Yildiz, A.B.; Yixuan, H.; Babu, R.P.; Hansen, T.C.; Eriksson, M.; Reddy, K.M.; Hedström, P. Design, Synthesis, Structure, and Stability of Novel Multi-Principal Element (Ti,Zr,Hf,W)C Ceramic with a Miscibility Gap. *J. Eur. Ceram. Soc.* **2022**, *42*, 4429–4435. [CrossRef]
21. Vorotilo, S.; Kiryukhantsev-Korneev, P.V.; Seplyarskii, B.S.; Kochetkov, R.A.; Abzalov, N.I.; Kovalev, I.D.; Lisina, T.G.; Zaitsev, A.A. (Ti,Cr)C-Based Cermets with Varied Nicr Binder Content via Elemental SHS for Perspective Cutting Tools. *Crystals* **2020**, *10*, 412. [CrossRef]
22. Borisov, Y.S.; Borisova, A.L.; Kolomytsev, M.V.; Masyuchok, O.P.; Timofeeva, I.I.; Vasilkovskaya, M.A. High-Velocity Air Plasma Spraying of (Ti, Cr)C–32 wt.% Ni Clad Powder. *Powder Metall. Met. Ceram.* **2005**, *56*, 305–315. [CrossRef]
23. Carvajal, R. Recent Advances in Magnetic Structure Determination by Neutron Powder Diffraction. *J. Phys. B* **1993**, *192*, 55–69. [CrossRef]
24. Rietveld, H.M. A Profile Refinement Method for Nuclear and Magnetic Structures. *J. Appl. Crystallogr.* **1969**, *2*, 65–71. [CrossRef]
25. Loshe, B.H.; Calka, A.; Wexler, D. Synthesis of TiC by Controlled Ball Milling of Titanium and Carbon. *J. Mater. Sci.* **2007**, *42*, 669–675. [CrossRef]
26. Arao, Y.; Tanks, J.D.; Aida, K.; Kubouchi, M. Exfoliation Behavior of Large Anionic Graphite Flakes in Liquid Produced by Salt-Assisted Ball Milling. *Processes* **2020**, *8*, 28. [CrossRef]
27. Hübler, D.; Gradt, T. Effect of Different Binders and Secondary Carbides on NbC Cermets. *Forsch. Ingenieurwes.* **2022**, *86*, 197–211. [CrossRef]
28. Cheng, Y.N.; Nie, W.Y.; Guan, R.; Jia, W.K.; Yan, F.G. Study on Damage Behavior of Carbide Tool for Milling Difficult-to-Machine Material Show Less. *Proc. Inst. Mech. Eng. Part C J. Mech. Eng. Sci.* **2018**, *233*, 735–747. [CrossRef]
29. Shon, I.J.; Oh, H.S.; Lim, J.W.; Kwon, H. Mechanical Properties and Consolidation of Binderless Nanostructured (Ti,Cr)C from Mechanochemically-Synthesized Powder by High-Frequency Induction Heating Sintering. *Ceram. Int.* **2013**, *39*, 9721–9726. [CrossRef]

30. Mohammed, S.M.A.K.; Chen, D.L. Carbon Nanotube-Reinforced Aluminum Matrix Composites. *Adv. Eng. Mater.* **2020**, *22*, 12–27. [CrossRef]
31. Zhu, Y.T.; Huang, J.Y.; Gubicza, J.; Ungar, T.; Wang, Y.M.; Ma, E.; Valiev, R.Z. Nanostructures in Ti Processed by Severe Plastic Deformation. *J. Mater. Res.* **2003**, *18*, 1908–1917. [CrossRef]
32. Mhadhbi, M.; Khitouni, M.; Escoda, L.; Suñol, J.J.; Dammak, M. Characterization of Mechanically Alloyed Nanocrystalline Fe(Al): Crystallite Size and Dislocation Density. *J. Nanometer.* **2010**, *2010*, 712407. [CrossRef]
33. Slater, J.C. Atomic Radii in Crystals. *J. Chem. Phys.* **1964**, *41*, 3199–3204. [CrossRef]
34. Zarrinfar, N.; Shipway, P.H.; Kennedy, A.R.; Saidi, A. Carbide Stoichiometry in TiC_x and Cu-TiC_x Produced by Self-Propagating High-Temperature Synthesis. *Scr. Mater.* **2002**, *46*, 121–126. [CrossRef]
35. Groß, H.; Ekici, Y.; Poschmann, M.; Croeneveld, D.; Dankwort, T.; Koenig, J.D.; Bensch, W.; Kienle, L. Does a Low Amount of Substituents Improve the Thermoelectric Properties of $Cr_{2-x}M_xS_3$ (M = Ti, V, Sn)? *J. Electron. Mater.* **2022**, *51*, 3510–3520. [CrossRef]
36. Suryanarayana, C. Mechanical Alloying: A Novel Technique to Synthesize Advanced Materials. *Research* **2019**, *2019*, 4219812. [CrossRef]
37. Kwon, H.; Jung, S.A.; Kim, W. (Ti,Cr)C Synthesized In Situ by Spark Plasma Sintering of TiC/Cr_3C_2 Powder Mixtures. *Mater. Trans.* **2015**, *56*, 264–268. [CrossRef]
38. Pradhan, B.; Ghosh, S.; Roy, D.; Samanta, L.K. Preparation of Nanocrystalline $CuAlFeS_2$-Mixed Chalcopyrite by High-energy Ball Milling. *Physica* **2006**, *33*, 66–68. [CrossRef]